JAET

Journal homepage: http://jae-tech.com

Journal of Applied Engineering & Technology

ISSN : 2523-6032 ISSN-L : 2523-2924

Simulation-Based Design and Evaluation of Temperature Insensitive Device for SiOC on Insulator Platform

Shehroz Jehangir[1,*], Umair Ahmed Korai[1], Abi Waqas[1]

[1]Department of Telecommunication Engineering, Mehran University of Engineering and Technology Jamshoro, 76200, Pakistan

*Corresponding Author
DOI: https://doi.org/10.55447/jaet.06.01.55

Abstract: Silicon Oxycarbide (SiOC) has emerged as an intriguing material platform in integrated photonics due to its large adjustable refractive index window and low absorption coefficient. Changes in composition can tailor its physical, optical, and chemical properties over a wide range of parameters. The building-block method to circuit simulation is a useful framework for extensively exploiting photonics potential in vast implementation of complex circuits. Due to the large thermo-optic coefficient of the silicon-on-insulator (SOI) platform's core material, temperature dependency is one of the SiOC platform's key problems. In this paper, we designed and tested a temperature insensitive optical sensor using SiOC on insulator in available simulator, which only propagates single mode through the waveguide. We were able to find the first mode propagation at 600 nm to 1200 nm waveguide widths with the constant height of 220 nm. The significance of MZI based simulated sensor is that it is completely temperature insensitive at 1550 nm wavelength. We also realized from our simulated device that above 1200 nm waveguide width, the device has multimode propagation capability.

Keywords: MZI, SiOC, thermo-optic coefficient, silicon-on-insulator platform.

1. Introduction

With its fascinating optical, physical, and chemical properties, SiOC has appeared as an intriguing material framework that can be customized by adjustments in structure over a wide window. In many fields it has been adopted and implemented, i.e., anode material for Li-ion cells, very low dielectric material for internal dielectrics, electroluminescence, photoluminescence and doped optical amplifiers for rare earth elements. One of the most developed and popular technologies for supporting big scale photonics integrated circuits (PICs) is silicon photonics [1–3]. To utilize the 2D material within PICs, we require to follow step by step process, and their exfoliated 2D ultrathin membranes or chemical vapor deposition grown are integrated on the dielectric substrates such as silica or silicon wafers [4, 5]. While using multiple deposition techniques throughout different pre- and post-deposition settings, SiOC thin films were prepared. SiOC technology for integrated photonics has been developed by different researchers. The transfer approaches used in this process are complex even though they are widespread nowadays [6]. Integrated photonics is the discipline in which by the

*Corresponding author: 19metlem04@students.muet.edu.pk

utilization of dielectric waveguides, the passive optical devices (i.e., interferometers, couplers, and so on) can be fabricated into a chip. The advancement of technology in integrated photonics has assisted in the deployment of complex photonic circuitry that incorporate multiple single-chip features, significant production quantities, and decreased manufacturing costs. Complex and lightweight materials have contributed to new applications and market prospects in recent years.

The PICs are anticipated to be rapidly implemented in the areas of optical communication. Breakthroughs in photonic integration allow complex photonic circuitry to be integrated, combining different features and functionality on a single chip, theoretically producing substantial production volumes and cheap production costs. The photonic community has utilized the benefits of incorporating optical circuits for biological use, narrow band filtering, optical signal processing, sensing, microwave photonic system etc., hence becoming mostly dominated in the telecom industry. One of the main limitations of the photonic integrated devices is its temperature dependency, which have opened the door for researchers to design an athermal devices [7, 8]. The functional components like high-speed modulators and broadband switches are demonstrated while using resonated cavities [9–12] or Mach-Zehnder Interferometer [13–17], but all these devices suffer from noteworthy performance degradation with the temperature variation because of high thermo-optic coefficient of the most used platforms, such as SOI, SiOC on insulator, and related materials [18, 19]. Even small temperature variations can cause a production of significant phase errors [20]. An all passive athermal SOI MZI which was based on standard silicon material common platform was introduced [21], whereas we used SiOC instead of silicon to design a temperature insensitive device. Our device solved the problem of temperature sensitivity using SiOC on insulator platform as discussed above. As silicon is compatible to CMOS, likewise SiOC is also compatible to CMOS. That is why we did research on SiOC on insulator for temperature. As for this paper [22], the thermos-optic coefficient of SiOC is very high, therefore a temperature insensitive device is required.

2. Background and Literature Review

One of the approaches proposed includes the use of polymer overlay cladding having a negative thermo-optic coefficient [23, 24]. One of the other approaches is the use of local heating to dynamically stabilize the proposed device. This can be done in several ways which includes using the direct silicon device heating by varying the bias current for an active device [25], using external heaters [26], or by using the silicon as the direct means for heating while keeping it as resistive material [27]. All the mentioned approaches are active and are required to have substantial power consumption and space, which accounts most often for the highest share in power budget of the silicon photonics which is state-of-art [28] and complex fabrication. Guha et.al. [29] proposed an approach to eradicate the temperature sensitivity of MZIs and achieved this by altering the thermo-optic effects through their length optimization and waveguide width of their interfering arms. They also demonstrated that the thermal spectral shift can also be brought down to near zero over a wide range of temperature and this was reported for the first time. Uenuma et.al. [30] projected a novel design for temperature independent silicon waveguide by applying an amalgamation of narrow and wide waveguides along with their lengths. Structure of waveguide was optimized to diminish the spectral phase shift of the filter at central wavelength of 1550 nm which owed to the temperature changes in environment. While using this design as a base, they also developed Mach–Zehnder interferometer optical filters on the substrates of SOI. Ye et al. [31] in order to reduce temperature shift proposed silicon waveguide filters by using negative thermo-optic coefficient polymer cladding for compensating the silicon material positive thermo-optic coefficient. An experimental integrated Mach-Zehnder interferometer is presented as a first example of PIC realized on high refractive index SiOC platform [32], whereas we introduced MZI based temperature insensitive sensor using SiOC. Abi et al. [33] proposed design and experimental authentication of the SiOC based devices i.e., waveguide and directional coupler for a waveguide dimension of 1300×200 nm^2 having gap of 1000

nm, whereas our research was based on 220 nm height of waveguide, and we introduced MZI based sensor using SiOC based waveguides. An ultra-sensitive temperature sensor is demonstrated [34] on the silicon-on-insulator (SOI) platform using cascaded Mach–Zehnder interferometers (MZIs). The measured sensitivity they found out about 21.9 times larger than available conventional silicon temperature sensors. The measured sensitivity is 1753.7 pm/°C from 27°C to 67°C, that is greater than any stated results on a silicon platform and is about 21.9 times greater than available conventional silicon temperature sensors.

3. Research Methodology

In this work, we utilized extensive use of SiOC on insulator using Lumerical Mode Solutions. The group and effective refractive index are calculated in this tool for the waveguide width ranges from 600 to 1200 nm for the constant height of 220 nm. The single mode operation is achieved using the above width range with a constant height of 220 nm, as shown in Fig. 1. After calculating the group and effective refractive indices of said waveguide width range, (1), (2), and (3) are evaluated theoretically and calculated the temperature sensitivity. It can be observed from the results section, discussed later, that appropriate selection of the length and widths of waveguide for upper and lower arms of MZI leads to the athermal device.

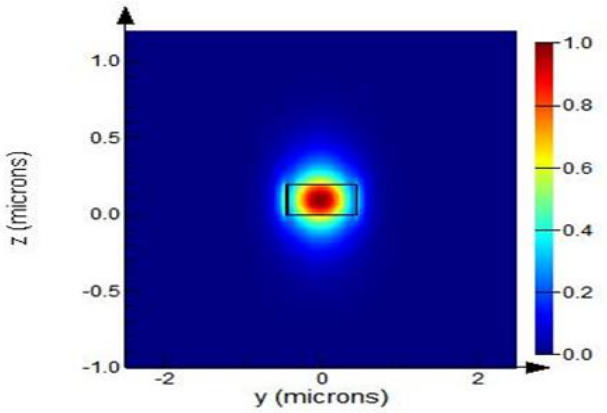

Fig. 1 - Single mode propagation of 900 nm width waveguide

Fig. 2 shows the flow chart of our work and how we obtained our data sets for MZI based device design.

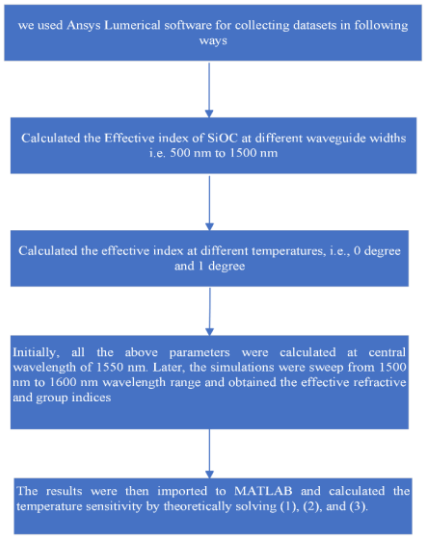

Fig. 2 - Flow chart of Research Methodology

3.1 Lumerical

Ansys Lumerical Mode Solution is a photonics simulation software that is used for precise evaluation of mesh and newest materials simulations. Lumerical also provides a vast script editing environment which enables for designers to do huge range simulations without manually adjusting values every time. We also used Lumerical Mode Solution editor to perform our simulations on different widths for huge number of points in wavelength range of 1500 nm to 1600 nm. Component-level and system-level simulations are available in Ansys Lumerical's full suite of photonics simulation and analysis tools to maximize performance, decrease physical prototype costs, and shorten time-to-market. Designers can now create small models that are tuned to leading foundry techniques thanks to improved design procedures. Fig. 3 shows the design of our SiOC based Waveguides.

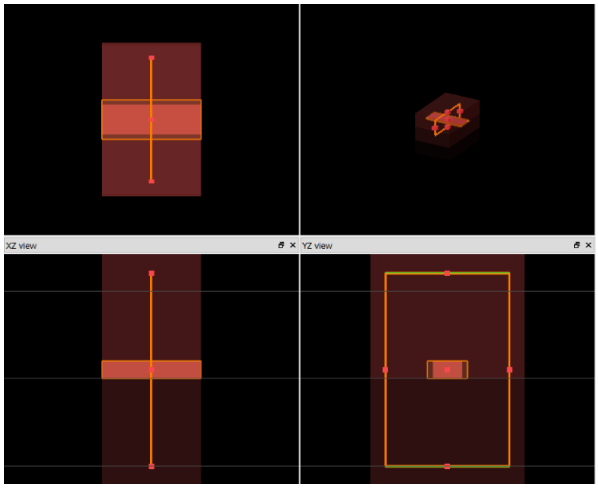

Fig. 3 - Design of SiOC Based Waveguide

3.2 MATLAB

MathWorks created MATLAB, a commercial multi-paradigm scripting languages and quantitative computing environment. The functions that MATLAB provides are plotting of data and functions, interfacing with other programming languages, development of user interfaces, implementation of algorithms, and matrix manipulations. In our research, we used MATLAB to develop an MZI based on equations of MZI and used temperature shift equations to evaluate the best 20 nm bandwidth range for our single mode waveguide widths datasets that we have developed through Lumerical Mode Solution scripting simulations. MATLAB allowed for plotting and evaluating of temperature shift values and effective index, as well as L and ΔL values of our equations in ease-of-use form for us to evaluate our results.

4. Results and Discussion

As we know that when second order mode's effective index of waveguide increases to value more than neff > 1.45 then it becomes multimode waveguide. So, in our research we evaluated and simulated only those waveguide widths which give single TE mode for SiOC on insulator platform. From Fig. 4 we can observe our MZI based temperature insensitive device and the waveguide made is of SiOC whereas the insulator platform is SiO2. The upper arm *W1* is adjusted from 600 nm to 1200 nm for our research to obtain datasets for our research through Lumerical software and lower arm *W2* is always kept lower than upper arm due to 0-degrees and 1-degrees temperature shift and according to equations as stated below. The response of our waveguide can be obtained from [21]:

$$m\lambda_0 = n_{eff1} . \Delta L + \Delta n_{eff} . L \quad (1)$$

Here n_{eff1} is the effective index of MZI wire waveguides; m is a parameter that indicates constructive interference at λ_0 and if it is half integer than it will result in destructive interference. The interference order (M) of the MZI can be written as [21]:

$$M = m - \Delta L \frac{dn_{eff1}}{d\lambda} - L \frac{d\Delta n_{eff}}{d\lambda} \quad (2)$$

The athermal MZI overall temperature sensitivity at any specified wavelength λ_0 can be written as [21]:

$$S = \frac{\Delta\lambda_0}{\Delta T} = \frac{\Delta L \frac{dn_{eff1}}{dT} + L \frac{d\Delta n_{eff}}{dT}}{M} \quad (3)$$

Because Silicon Oxycarbide has a positive thermo-optic coefficient, therefore the first term of (3) is always positive, therefore the upper arm width is always kept higher than lower arm because otherwise the thermo-optic coefficient values will end up as negative and cannot be measured in MATLAB equation calculation and find command.

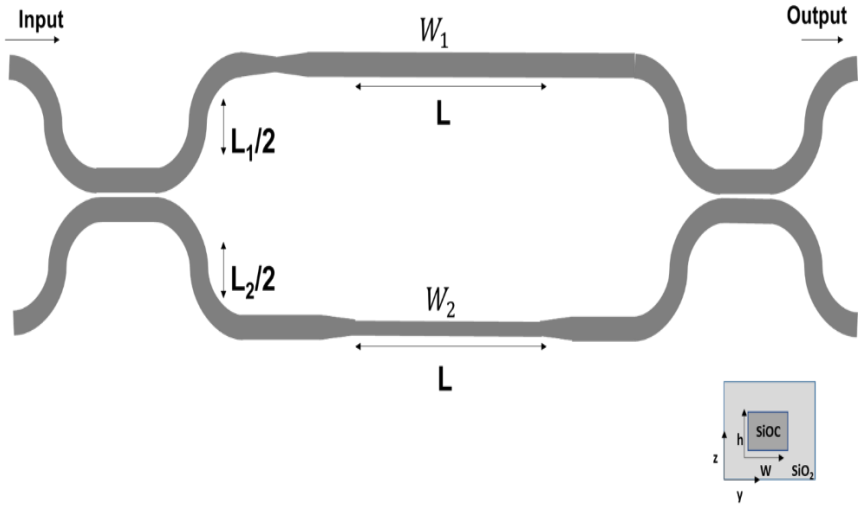

Fig. 4 - Schematic Diagram of proposed MZI sensor

We simulated our waveguide designed from Silicon oxycarbide on insulator platform with SiO2 as substrate at waveguide widths of 500 nm to 1500 nm, where the height *h* of waveguide was fixed at 220 nm, and the width *W* was varied from 500 nm to 1500 nm. After simulating modes of waveguide from Lumerical Mode Solution, we were able to find out that as the width was increased by increment of 100 nm, the effective index of waveguide modes kept increasing, until we reached the 1200 nm waveguide width at which the first mode propagation of SiOC based waveguide has reached its limit. After 1200nm, we were not able to obtain single mode propagation for our SiOC based waveguide and hence our scope of research was focused on 500nm to 1200nm waveguide widths datasets that contained values of n_{eff} and group index (n_g) for the wavelength ranges from 1500 nm to 1600 nm. Fig. 5 shows the perfect single mode propagation of SiOC based waveguide when its width *w* is kept at 600 nm with fixed 220 nm height *h*.

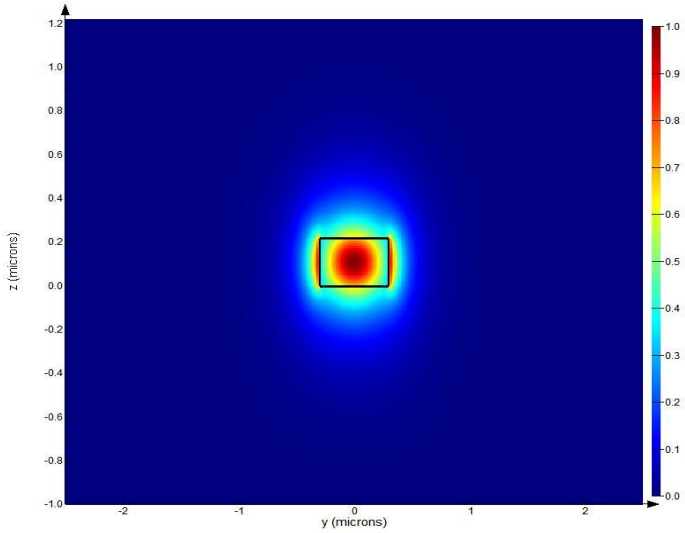

Fig. 5 - Single mode of 600 nm width waveguide

Fig. 6 shows the mode profile of the SiOC waveguide with width as 1200 nm and height of 220 nm. This mode profile is the 2nd order mode of the waveguide which is about to propagate. But as the effective index of the 2nd order TE mode is less than the cutoff value, hence it will not be considered as active mode and the waveguide is considered as single mode waveguide. Therefore, the waveguide width until 1200 nm gives the first order operation and the datasets of n_{eff} is considered up until this width with a constant height of 220 nm.

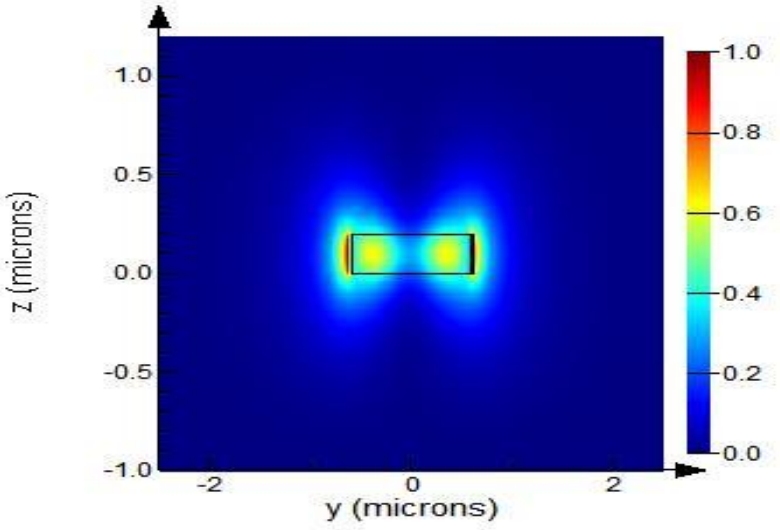

Fig. 6 – Single mode of 1200 nm width Waveguide

From table 1 it can be observed that the effective index of 1200 nm in mode list has a value of 1.444604 and it still acts as a single mode waveguide for optical propagation. It was also observed that if we increased the width more than 1200 nm, then 2nd order TE mode will start to propagate in to waveguide and it will be considered as the multimode waveguide.

Table 1 – Mode List of 1200 nm Width Waveguide

Mode list

mode #	effective index	wavelength (µm)	loss (dB/cm)	TE polarization fraction (Ey)	waveguide TE/TM fraction (%)
1	1.629191	1.5	0.00000	100	93.52 / 85.8
2	1.498005	1.5	0.00000	0	93.28 / 96.89
3	1.444604	1.5	0.00000	95	88.09 / 92.02
4	1.423053	1.5	0.00000	0	99.23 / 94.81

We created cases while fixing *W1* upper arm value at 600 nm to 1200 nm and obtained temperature shift of 20 nm bandwidth starting from 1540 nm to 1560 nm. We theoretically solved (1), (2), and (3) to calculate temperature sensitivity in pm/k for our analysis and found the possible temperature shift of at 1540 nm to 1560 nm wavelength for *W1* = 1200 nm and *W2* = 1100 nm widths of MZI arms, under the required range of -1 to +1 pm/°k as shown in Fig. 7. Here, our MZI based device is temperature insensitive at 1550 nm wavelength as we can observe from Fig. 7.

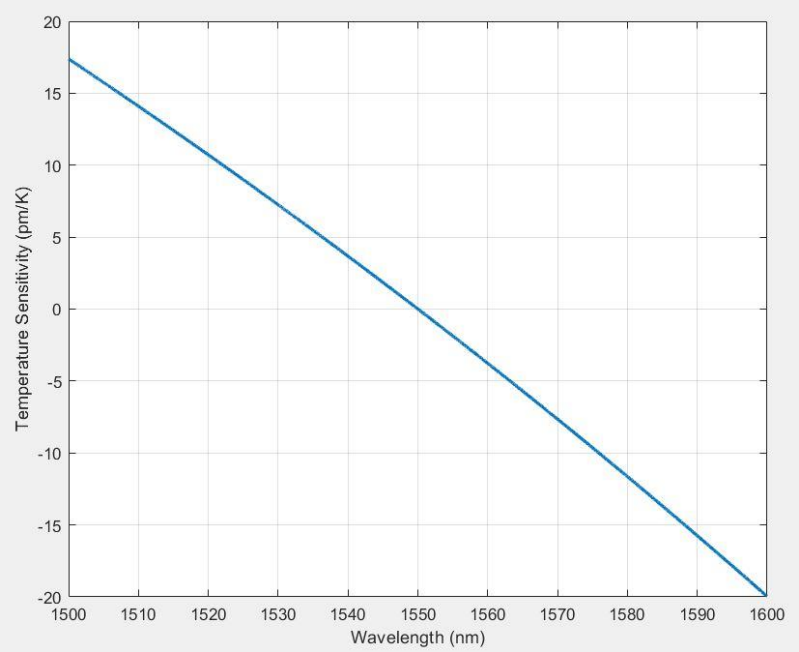

Fig. 7 - Temperature shift of w1=1200 nm, w2=1100 nm of MZI based device.

5. Conclusion

From the simulation, we came to found out that, from 600 nm to 1200 nm the effective index of mode is less than 1.47 and hence they propagate single modes through them. The waveguide widths from 600 nm to 1200 nm can be utilized for single mode propagation through waveguide based on SiOC on insulator platform. Through these waveguide dimensions we designed MZI SiOC based temperature insensitive device on insulator platform which was temperature insensitive at 1550 nm range when upper arm width is 1200 nm and lower arm width is kept at 1100 nm respectively. Our proposed MZI based temperature insensitive device is based on SiOC technology as compared to SOI technology of majority of existing devices. Our proposed design is the first temperature insensitive device using SiOC on insulator platform as per our knowledge and research. From our research it can be concluded that SiOC technology can be employed for temperature insensitive

applications and can be further experimented for reaching better thermos optic coefficient demands ranging from 10 nm to 100 nm bandwidths.

References

[1]. Thomson, D., Zilkie, A., Bowers, J. E., Komljenovic, T., Reed, G. T., Vivien, L., ... & Nedeljkovic, M. (2016). Roadmap on silicon photonics. Journal of Optics, 18(7), 073003.

[2]. Soref, R. (2006). The past, present, and future of silicon photonics. IEEE Journal of selected topics in quantum electronics, 12(6), 1678-1687.

[3]. Jalali, B., & Fathpour, S. (2006). Silicon photonics. Journal of lightwave technology, 24(12), 4600-4615.

[4]. Liu, M., Yin, X., Ulin-Avila, E., Geng, B., Zentgraf, T., Ju, L., ... & Zhang, X. (2011). A graphene-based broadband optical modulator. Nature, 474(7349), 64-67.

[5]. Gu, T., Petrone, N., McMillan, J. F., van der Zande, A., Yu, M., Lo, G. Q., ... & Wong, C. W. (2012). Regenerative oscillation and four-wave mixing in graphene optoelectronics. Nature Photonics, 6(8), 554-559.

[6]. Lin, H., Song, Y., Huang, Y., Kita, D., Deckoff-Jones, S., Wang, K., ... & Hu, J. (2017). Chalcogenide glass-on-graphene photonics. Nature Photonics, 11(12), 798-805.

[7]. Miller, D. A. (2000). Rationale and challenges for optical interconnects to electronic chips. Proceedings of the IEEE, 88(6), 728-749.

[8]. Alduino, A., & Paniccia, M. (2007). Wiring electronics with light. Nature Photonics, 1(3), 153-155.

[9]. Xu, Q., Schmidt, B., Pradhan, S., & Lipson, M. (2005). Micrometre-scale silicon electro-optic modulator. nature, 435(7040), 325-327.

[10]. Manipatruni, S., Xu, Q., Schmidt, B., Shakya, J., & Lipson, M. (2007, October). High speed carrier injection 18 Gb/s silicon micro-ring electro-optic modulator. In LEOS 2007-IEEE Lasers and Electro-Optics Society Annual Meeting Conference Proceedings (pp. 537-538). IEEE.

[11]. Watts, M. R., Trotter, D. C., Young, R. W., & Lentine, A. L. (2008, September). Ultralow power silicon microdisk modulators and switches. In 2008 5th IEEE international conference on group IV photonics (pp. 4-6). IEEE.

[12]. You, J. B., Park, M., Park, J. W., & Kim, G. (2008). 12.5 Gbps optical modulation of silicon racetrack resonator based on carrier-depletion in asymmetric pn diode. Optics express, 16(22), 18340-18344.

[13]. Liu, A., Jones, R., Liao, L., Samara-Rubio, D., Rubin, D., Cohen, O., ... & Paniccia, M. (2004). A high-speed silicon optical modulator based on a metal–oxide–semiconductor capacitor. Nature, 427(6975), 615-618.

[14]. Liu, A., Liao, L., Rubin, D., Nguyen, H., Ciftcioglu, B., Chetrit, Y., ... & Paniccia, M. (2007). High-speed optical modulation based on carrier depletion in a silicon waveguide. Optics express, 15(2), 660-668.

[15]. Green, W. M., Rooks, M. J., Sekaric, L., & Vlasov, Y. A. (2007). Ultra-compact, low RF power, 10 Gb/s silicon Mach-Zehnder modulator. Optics express, 15(25), 17106-17113.

[16]. Marris-Morini, D., Vivien, L., Fédéli, J. M., Cassan, E., Lyan, P., & Laval, S. (2008). Low loss and high speed silicon optical modulator based on a lateral carrier depletion structure. Optics express, 16(1), 334-339.

[17]. Spector, S. J., Geis, M. W., Zhou, G. R., Grein, M. E., Gan, F., Popović, M. A., ... & Lyszczarz, T. M. (2008). CMOS-compatible dual-output silicon modulator for analog signal processing. Optics Express, 16(15), 11027-11031.

[18]. Cocorullo, G., & Rendina, I. (1992). Thermo-optical modulation at 1.5 mu m in silicon etalon. Electronics Letters, 28(1), 83-85.

[19]. Varshni, Y. P. (1967). Temperature dependence of the energy gap in semiconductors. physica, 34(1), 149-154.

[20]. Cocorullo, G., & Rendina, I. (1992). Thermo-optical modulation at 1.5 mu m in silicon etalon. Electronics Letters, 28(1), 83-85.

[21]. Korai, U. A., Bermello, A. H., Strain, M. J., Glesk, I., & Velasco, A. V. (2019). Design of an athermal interferometer based on tailored subwavelength metamaterials for on-chip microspectrometry. IEEE Photonics Journal, 11(6), 1-11.

[22]. Memon, F. A., Morichetti, F., & Melloni, A. (2018). High thermo-optic coefficient of silicon oxycarbide photonic waveguides. ACS Photonics, 5(7), 2755-2759.

[23]. Han, M., & Wang, A. (2007). Temperature compensation of optical microresonators using a surface layer with negative thermo-optic coefficient. Optics letters, 32(13), 1800-1802.

[24]. Teng, J., Dumon, P., Bogaerts, W., Zhang, H., Jian, X., Han, X., ... & Baets, R. (2009). Athermal Silicon-on-insulator ring resonators by overlaying a polymer cladding on narrowed waveguides. Optics express, 17(17), 14627-14633.

[25]. Manipatruni, S., Dokania, R. K., Schmidt, B., Sherwood-Droz, N., Poitras, C. B., Apsel, A. B., & Lipson, M. (2008). Wide temperature range operation of micrometer-scale silicon electro-optic modulators. Optics letters, 33(19), 2185-2187.

[26]. Amatya, R., Holzwarth, C. W., Popovic, M. A., Gan, F., Smith, H. I., Kartner, F., & Ram, R. J. (2007, May). Low power thermal tuning of second-order microring resonators. In 2007 Conference on Lasers and Electro-Optics (CLEO) (pp. 1-2). IEEE.

[27]. Watts, M. R., Zortman, W. A., Trotter, D. C., Nielson, G. N., Luck, D. L., & Young, R. W. (2009, May). Adiabatic resonant microrings (ARMs) with directly integrated thermal microphotonics. In Conference on Lasers and Electro-Optics (p. CPDB10). Optical Society of America.

[28]. Dokania, R. K., & Apsel, A. B. (2009, May). Analysis of challenges for on-chip optical interconnects. In Proceedings of the 19th ACM Great Lakes symposium on VLSI (pp. 275-280).

[29]. Guha, B., Gondarenko, A., & Lipson, M. (2010). Minimizing temperature sensitivity of silicon Mach-Zehnder interferometers. Optics express, 18(3), 1879-1887.

[30]. Uenuma, M., & Motooka, T. (2009). Temperature-independent silicon waveguide optical filter. Optics letters, 34(5), 599-601.

[31]. Winnie, N. Y., Michel, J., & Kimerling, L. C. (2008). Athermal high-index-contrast waveguide design. IEEE Photonics Technology Letters, 20(11), 885-887.

[32]. Memon, F. A., Morichetti, F., Cantoni, M., Somaschini, C., Asa, M., Bertacco, R., ... & Melloni, A. (2020). Silicon oxycarbide platform for integrated photonics. Journal of Lightwave Technology, 38(4), 784-791.

[33]. Waqas, A., Memon, F. A., & Korai, U. A. (2020). Experimental validation of a building block of passive devices and stochastic analysis of PICs based on SiOC technology. Optics Express, 28(15), 21420-21431.

[34]. Ding, Z., Dai, D., & Shi, Y. (2021). Ultra-sensitive silicon temperature sensor based on cascaded Mach–Zehnder interferometers. Optics Letters, 46(11), 2787-2790.